Mol Cell Biochem (2017) 428:171–178
DOI 10.1007/s11010-016-2927-3

Albendazole inhibits HIF-1α-dependent glycolysis and VEGF expression in non-small cell lung cancer cells

Fang Zhou[1] · Jin Du[2] · Jianjun Wang[1]

Received: 18 August 2016 / Accepted: 21 December 2016 / Published online: 7 January 2017

Abstract Albendazole (ABZ) has an anti-tumor ability and inhibits HIF-1α activity. HIF-1α is associated with glycolysis and vascular endothelial cell growth factor (VEGF) expression, which plays an important role in cancer progression. These clues indicate that ABZ exerts an anti-cancer effect by regulating glycolysis and VEGF expression. The aim of this study is to clarify the effects of ABZ on non-small cell lung cancer (NSCLC) cells and explore the underlying molecular mechanisms. The expression levels of HIF-1α and VEGF were detected using western blot analysis, and the effect of ABZ on glycolysis was evaluated by measuring the relative activities of hexokinase (HK), pyruvate kinase (PK), and lactate dehydrogenase (LDH) and detecting the production of lactate in A549 and H1299 cells. The results showed that ABZ decreased the expression levels of HIF-1α and VEGF and suppressed glycolysis in under hypoxia, but not normoxic condition. Inhibiting HIF-1α also suppressed glycolysis and VEGF expression. Additionally, ABZ inhibited the volume and weight, decreased the relative activities of HK, PK, and LDH, and reduced the levels of HIF-1α and VEGF of A549 xenografts in mouse models. In conclusion, ABZ inhibited growth of NSCLC cells by suppressing HIF-1α-dependent glycolysis and VEGF expression.

Keywords Albendazole · HIF-1α · Glycolysis · VEGF · Non-small cell lung cancer

✉ Fang Zhou
fzhouzz@126.com

[1] Department of Oncology, Huaihe Hospital of Henan University, No. 8 Baobei Road, Kaifeng 475000, China

[2] Department of Respiration, Huaihe Hospital of Henan University, Kaifeng 475000, China

Introduction

Lung cancer was the most commonly diagnosed cancers among men and the second most commonly diagnosed cancers among women in 2015 in China [1]. According to the data from American Cancer Society, more than a quarter of all cancer deaths are due to lung cancer [2]. Most lung cancers are non-small cell lung cancer (NSCLC), so it is meaningful to find out drugs that can be candidates for the anti-cancer therapy of NSCLC.

Albendazole (ABZ) is a broad spectrum benzimidazole carbamate anthelminthic with low toxicity and is widely used in human and animals [3]. ABZ inhibits helminths cell proliferation by binding to β-tubulin and inhibiting microtubule polymerization [4]. As a result, it reduces parasite survival and reproduction. In 1985, it was reported that benzimidazole carbamates had anti-tumor effect in mouse leukaemia cells [5]. Subsequently, many researchers studied the anti-tumor activity of ABZ and found that it had anti-proliferative properties in many cancer cells, such as hepatocellular carcinoma cells [6], colorectal cancer cells [7]. Phase I clinical trial has been done to determine maximum tolerated dose of oral albendazole in patients with advanced cancer [8]. However, the inhibitory mechanism of ABZ on NSCLC remains to be illustrated.

Tumor cells must change their metabolic way to meet their increasing needs for growth and proliferating. There is a famous phenomenon which is called Warburg effect in tumor glycometabolism. It describes the phenomenon that most cancer cells generate ATP by a high rate of glycolysis converting glucose to lactate, rather than metabolizing glucose by oxidative phosphorylation, even when oxygen is plentiful [9, 10]. Due to Warburg effect, tumor cells require much more glucose than normal cells and

have highly active glycolysis. Lactate generated by glycolysis acidizes cells and benefits tumor.

Hypoxia-inducible factor-1α (HIF-1α) is the most important cell transcriptional activator in response to hypoxia and regulates a series of enzymes expression in the glycolytic pathway, such as succinate dehydrogenase [11], fumarate hydratase [11], pyruvate dehydrogenase kinases [11, 12], hexokinase (HK) [12], glucose transporters GLUT1 and GLUT3 [12, 13]. By anaerobic glycolysis, tumors metabolize glucose to lactate and survive in hypoxia environment. Under normoxic and iron-replete conditions, the protein expression of HIF-1α in cells is not detectable due to its rapid degradation [14]. However, the degradation is weak under hypoxia condition and results in the accumulation of HIF-1α in cells. Hyperactive metabolism in tumor cells increases oxygen consumption and leads to hypoxia. As a result, HIF-1α is accumulated in anoxic tumor cells. HIF-1α binds to vascular endothelial cell growth factor (VEGF) gene promoter and induces VEGF expression and angiogenesis, subsequently [15]. VEGF, usually overexpressed in NSCLC, is one of the most specific and crucial regulators of angiogenesis [16, 17], which suggests that targeting VEGF expression may an effective approach for NSCLC treatment. In this study, we explored the molecular mechanisms involving in the inhibition of glycolysis and VEGF expression affected by ABZ. These findings offered new insights into our understanding of the mechanisms underlying the anti-tumor function of ABZ.

Materials and methods

Cell culture and treatment

NSCLC A549 and H1299 cells were obtained from American Type Culture Collection (ATCC; Rockville, MD, USA), cultured in DMEM medium (Gibco, Grand Island, NY, USA), and supplemented with 10% FBS and 100 U/ml penicillin and 100 μg/ml streptomycin (Gibco) at 37 °C in a 5% CO_2 incubator. Cells were digested using 0.25% trypsin and passaged at 80–90% confluence. Before treatment, cells were allowed to attach the surface for 24 h. Cells were incubated with $CoCl_2$ (300 μM) or DFX (0, 100, 200 μM) in the presence or absence of ABZ (500 nM) for 24 h, followed by the western blot analysis, qRT-PCR, enzyme activity measurement, and lactate detection. Cells were exposed to PX-478 (0, 20, and 50 μM) in the presence or absence of DFX (200 μM) for 24 h, and the levels of HIF-1α mRNA, HIF-1α protein, and VEGF protein, the enzyme activities of HK, PK, and lactate dehydrogenase (LDH), and production of lactate were determined.

HK, PK, and LDH activities and lactate content measurements

Cells were inoculated in 6-well plates. After drug treatment, cells were digested with 0.25% trypsin and washed with PBS. Cell suspension was homogenized on ice. Protein concentration in homogenate was quantified by the BCA Protein Assay Kit (Thermo Fisher Scientific). HK, PK, and LDH activities and lactate content were measured by colorimetric assay using specific test kit bought from Solarbio (Beijing, China) according to the manufacturer's suggestions. The absorbance of HK and PK was measured at 340 nm and the absorbance of LDH was measured at 450 nm. The activities of HK, PK, and LDH were calculated according to the manufacturer's suggestions. The activity of HK, PK, and LDH in control group was normalized to 1.0.

Quantitative real-time polymerase chain reaction (qRT-PCR)

Total RNA was isolated from treated cancer cells using Trizol reagent (Tiangen, China) according to the manufacturer's instructions. Concentration and purity of total RNA samples were determined using the Nanodrop2000 (Thermo Scientific, Wilmington, DE, USA). Up to 5 μg of RNA was reverse transcribed into cDNA using the miScript II Reverse Transcription Kit (Qiagen, Germany) according to the manufacturer's protocols. The following primers were used for RT-PCR: HIF-1α (forward: 5′-TGC TCA TCA GTT GCC ACT TC-3′, reverse: 5′-CCA AGC AGG TCA TAG GTG GT-3′), and β-actin (forward: 5′-CTC CAT CCT GGC CTC GCT GT-3′, reverse: 5′-GCT GTC ACC TTC ACC GTT CC-3′). RT-PCR was performed using a miScript SYBR Green PCR Kit (Qiagen). β-actin mRNA was used as the reference gene to normalize the gene expression. Relative levels of mRNA were calculated using $2^{-\Delta\Delta Ct}$ method. All reactions were performed in triplicate.

Western blot analysis

For protein analysis, harvested cell pellets were lysed in RIPA lysis buffer (Beyotime, Haimen, China) supplemented with 1 mM PMSF. Cell lysates were centrifuged at 12,000×*g* at 4 °C for 5 min, and concentration of proteins in supernatant was quantified by the BCA Protein Assay Kit (Thermo Fisher Scientific). Samples with equal proteins were electrophoresed with SDS-PAGE and transferred to PVDF membrane. The membrane was blocked with 5% skim milk and incubated with monoclonal anti-HIF-1α antibody (Abcam, Cambridge, UK) or anti-VEGF antibody (Santa Cruz Biotechnology, Santa Cruz, CA, USA) for 2 h at room temperature, and then with HRP-conjugated

goat anti-rabbit IgG (Abcam) for 1 h. β-actin was used as an internal control. Proteins were visualized by ECL (Beyotime).

Xenograft tumor model

Four-to-five-week-old male athymic nude BALB/c mice (SLAC Laboratory, Shanghai, China) were used in this study. All mice were housed in a pathogen-free environment with *ad arbitrium* supply of water and food according to the guideline of Animal Care and Ethics Committee of Henan University (Kaifeng, China), and all experiments were performed in accordance with the protocols approved by the committee of Huaihe Hospital of Henan University. A549 xenografts were developed by subcutaneous injection of the A549 cells (2×10^6 cells per animal) into the flank of nude mice. The mice were randomly divided into two groups of 6 animals. Group 1 (the control group) received vehicle and Group 2 (the ABZ group) was administered 50 mg/kg of ABZ. Both groups received the treatment intraperitoneally every 3 days. Tumor growth was monitored by caliper, and tumor volumes were calculated every 5 days using the formula: Tumor volume = length × width^2/2. After 20 days, the animals were sacrificed and the tumors were harvested and weighted. Tumor tissues were stored at −80 °C for subsequent RNA and protein extraction and enzyme activity measurements.

Data statistics

All data were analyzed using student's *t* test or one-way analysis of variance (ANOVA). Data were considered to be statistically significant if $P<0.05$.

Results

ABZ inhibits hypoxia-induced HIF-1α expression and VEGF expression in NSCLC cells

VEGF is a specific and crucial regulator of angiogenesis, which is promoted by HIF-1α and is a key process involved in tumor progression [18–20]. In order to examine whether ABZ inhibits expression of HIF-1α and VEGF in A549 cells, we treated cells with $CoCl_2$, a hypoxia-mimetic agent, in the presence or absence of ABZ for 24 h. HIF-1α mRNA and protein expression levels of HIF-1α and VEGF were detected by western blot. The results showed that ABZ did not change the expression of HIF-1α mRNA and protein levels of HIF-1α and VEGF in A549 cells. $CoCl_2$ significantly increased the expression of HIF-1α mRNA and protein levels of HIF-1α and VEGF, which could be reduced by ABZ in A549 cells (Fig. 1a–d). To confirm the above effects of ABZ, A549 cells were treated with different concentration of DFX, another hypoxia-mimetic agent, in the presence or absence of ABZ for 24 h. As shown in Fig. 1e–h, DFX elevated the expression of HIF-1α mRNA and protein levels of HIF-1α and VEGF in A549 cells. Nevertheless, ABZ inhibited DFX-induced HIF-1α and VEGF expression in A549 cells. Similar findings were obtained in another NSCLC cell line H1299 (Fig. 1i–l). Collectively, our data revealed that ABZ had an ability to inhibit hypoxia-induced HIF-1α and VEGF expression.

ABZ inhibits hypoxia-induced glycolysis in NSCLC cells

Glycolysis is a major energy source in tumor and HIF-1α affects glycolysis by regulating a serious enzyme related to the glycolytic pathway [11]. To clarify whether ABZ had an effect on cellular glycolysis, A549 cells were treated with $CoCl_2$ in the presence or absence of ABZ for 24 h. Relative activities of HK, PK, LDH, and the lactate production were measured by colorimetric analysis. As shown in Fig. 2a–d, ABZ inhibited $CoCl_2$-induced activities of HK, PK, LDH, and lactate production in A549 cells. To confirm the above effects of ABZ, we also studied the effects of ABZ on DFX-induced glycolysis in A549 and H1299 cells. As expected, ABZ inhibited DFX-induced activities of HK, PK, LDH, and production of lactate in A549 (Fig. 2e–h) and H1299 (Fig. 2i–l) cells. Since HK, PK, and LDH are important enzymes in glycolysis and lactate is the major product of glycolysis, the result indicated that ABZ inhibited the glycolysis pathway in NSCLC cells.

Blocking HIF-1α inhibits glycolysis and VEGF expression

To confirm whether glycolysis and VEGF expression were regulated by HIF-1α, A549 cells were treated with 20 and 50 μM of PX-478, a HIF-1α inhibitor, for 24 h under hypoxia. We found that expression levels of HIF-1α mRNA and protein levels of HIF-1α and VEGF were declined with the increase of PX-478 concentration (Fig. 3a–d), indicating that blocking HIF-1α inhibited VEGF expression in NSCLC A549 cells. The relative activities of HK, PK, LDH, and the production of lactate were also decreased in the presence of PX-478 (Fig. 3e–h), suggesting that blocking HIF-1α inhibited glycolysis in NSCLC A549 cells.

ABZ inhibits A549 xenograft growth in vivo

We further examined the effect of ABZ on HIF-1α and VEGF expression and glycolysis in A549 xenografts in nude mice. The mice were randomly divided into two groups of 6 animals. The control group received vehicle

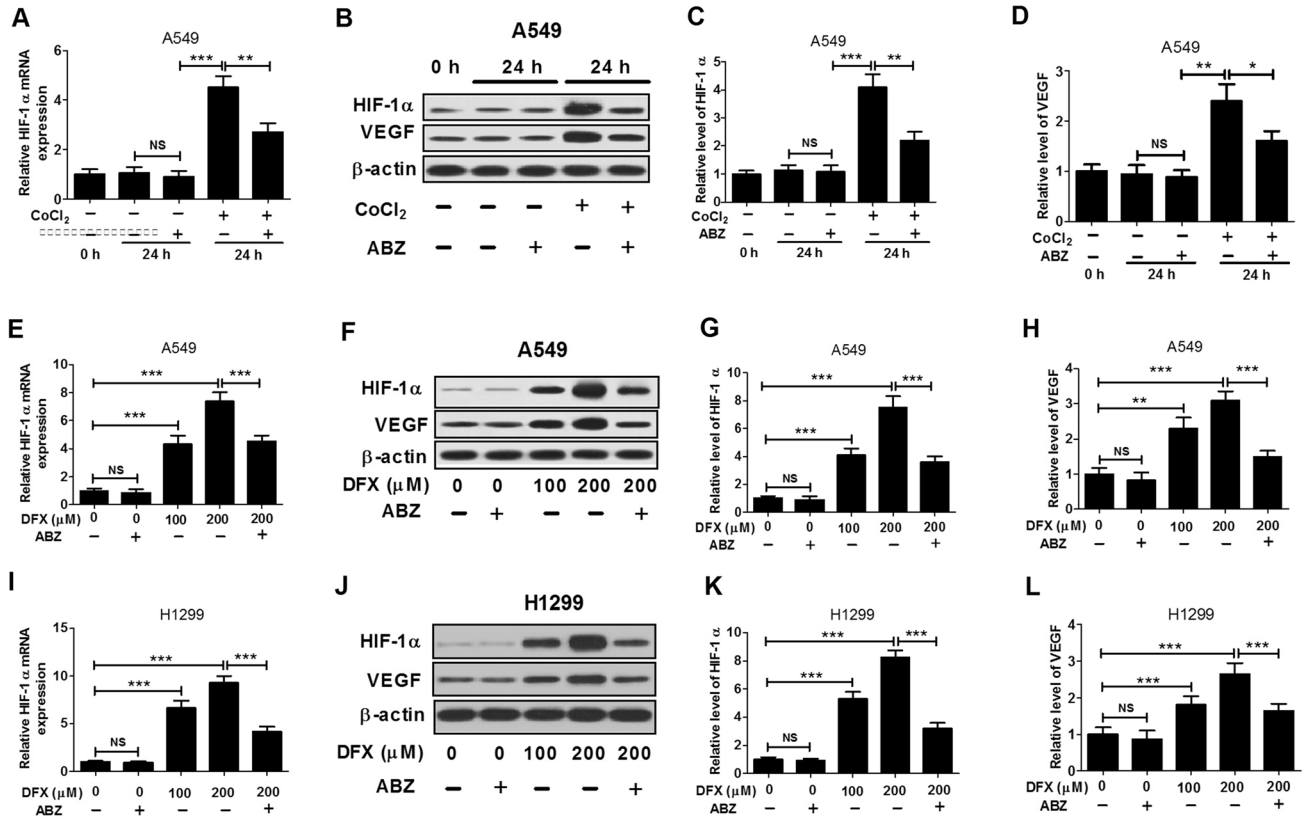

Fig. 1 ABZ inhibited hypoxia-induced HIF-1α and VEGF expression in A549 cells. **a–d** ABZ inhibited $CoCl_2$-induced HIF-1α mRNA expression and the protein levels of HIF-1α and VEGF. A549 cells were treated with 300 μM of $CoCl_2$ in the presence or absence of 500 nM of ABZ for 24 h. HIF-1α mRNA was detected by qRT-PCR, and protein expression levels of HIF-1α and VEGF were detected using western blot. ABZ inhibited DFX-induced HIF-1α expression and VEGF expression A549 (**e–h**) and H1299 (**i–l**) cells. Cells were treated with different concentrations of DFX (0, 100, and 200 μM) for 24 h. To assess the effect of ABZ on DFX-induced HIF-1α expression and VEGF expression, cells were co-incubated with 200 μM of DFX and 500 nM of ABZ for 24 h, followed by qRT-PCR and western blot analysis. Data are shown as mean ± standard deviation (SD; $n = 4$). *NS* not significant. $^{*}P < 0.05$, $^{**}P < 0.01$, $^{***}P < 0.001$

and the ABZ group was administered 50 mg/kg of ABZ. As illustrated in Fig. 4a, b, ABZ significantly inhibited tumor volume and weight in nude mice. ABZ treatment suppressed the expression of HIF-1α mRNA compared with the control group (Fig. 4c). The expression levels of HIF-1α and VEGF in A549 xenografts in the ABZ group were decreased compared with those in the control group (Fig. 4d). Furthermore, ABZ reduced the enzyme activities of HK, PK, and LDH compared with the control group (Fig. 4e). Taken together, these findings displayed that ABZ inhibited glycolysis and VEGF expression in vivo.

Discussion

ABZ has a wide effect on tumor development, such as inhibiting tumor growth, suppressing proliferation, arresting cell cycle, and promoting cells apoptosis [21–23]. Angiogenesis, an essential process for tumor growth, offers nutrient for tumor, takes metabolic waste away, and provides support for tumor spread and metastasis, and tumor frequently overexpresses pro-angiogenic factors, such as VEGF, for their progression [24–26]. Our result showed that ABZ inhibited hypoxia-induced accumulation of HIF-1α and VEGF expression. Noorani et al. [27] reported that nanoscale ABZ enhanced the anti-angiogenic property by inhibition of VEGF in ovarian cancer in both in vitro and in vivo models. Pourgholami et al. [28] found that tumoral HIF-1α and VEGF protein levels were highly suppressed in ABZ-treated mice. ABZ abolished tumor angiogenesis and ascites formation by inhibiting VEGF production in nude mice-bearing OVCAR-3 peritoneal tumors [29]. We speculated that the reduced VEGF expression is the result of ABZ-induced HIF-1α inhibition.

HIF1α has been suggested to be overexpressed in NSCLC and targeting the HIF pathway may prove of importance in the treatment of NSCLC [30]. $CoCl_2$ and DFX can block the HIF-1α degradation thus inducing the accumulation of HIF-1α and angiogenesis in tumor cells [31]. Borcar et al. found that $CoCl_2$ and DFX increased

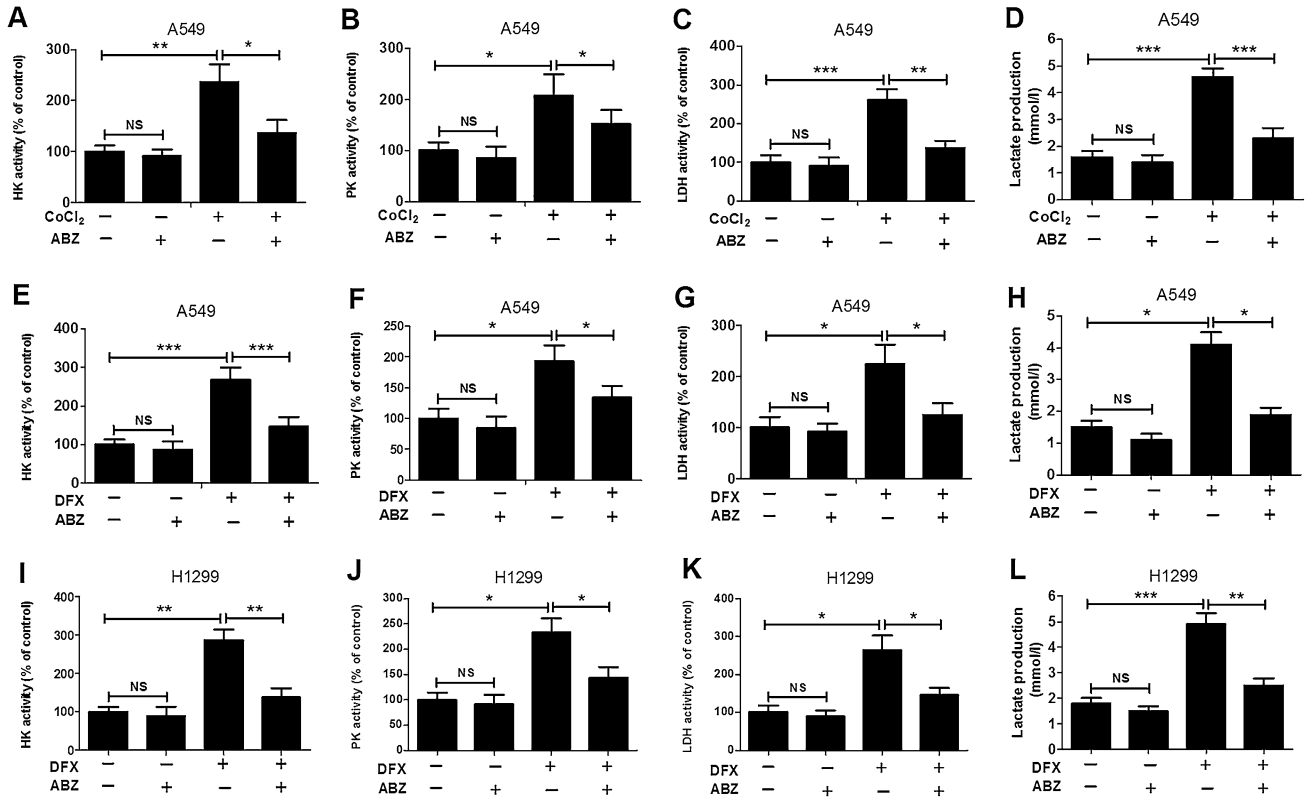

Fig. 2 ABZ inhibited hypoxia-induced glycolysis in A549 cells. **a–d** ABZ inhibited $CoCl_2$-induced activities of HK, PK, and LDH and lactate production in A549 cells. A549 cells were treated with 300 μM of $CoCl_2$ in the presence or absence of 500 nM of ABZ for 24 h. The activities of HK, PK, and LDH and lactate production were detected by colorimetric assay using specific test kit. ABZ inhibited DFX-induced activities of HK, PK, and LDH and lactate production in A549 (**e–h**) and H1299 (**i–l**) cells. Cells were treated with 200 μM of DFX in the presence or absence of 500 nM of ABZ for 24 h. Data are shown as mean ± standard error (SEM; $n = 3$). *HK* hexokinase, *PK* pyruvate kinase, *LDH* lactate dehydrogenase. *NS* not significant. $^{*}P < 0.05$, $^{**}P < 0.01$, $^{***}P < 0.001$

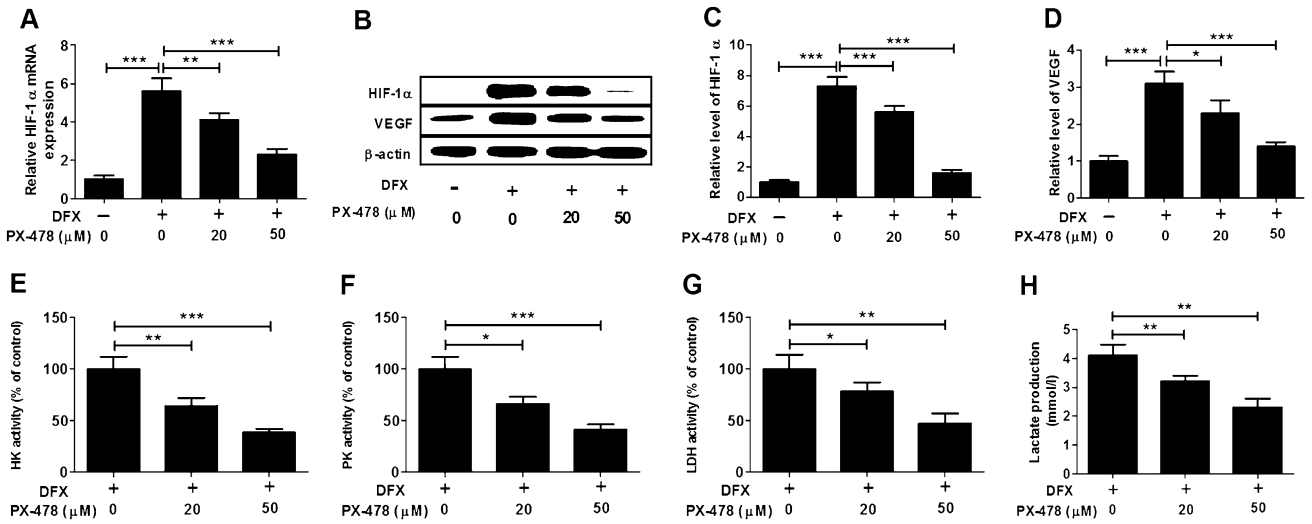

Fig. 3 Blocking HIF-1α inhibited glycolysis and VEGF expression. **a–d** PX-478, a HIF-1α inhibitor, significantly inhibited HIF-1α and VEGF expression. A549 cells were treated with 200 μM of DFX and different concentrations of PX-478 for 24 h. HIF-1α mRNA was detected using qRT-PCR and protein expression levels of HIF-1α and VEGF were detected using western blot. Data are shown as mean ± SD (n = 4). $^{*}P < 0.05$, $^{**}P < 0.01$, $^{***}P < 0.001$. **e–h** PX-478 inhibited DFX-induced activities of HK, PK, and LDH and lactate production in A549 cells. A549 cells were treated with 200 μM of DFX and different concentrations of PX-478 for 24 h. Data are shown as mean ± SEM ($n = 3$). *HK* hexokinase, *PK* pyruvate kinase, *LDH* lactate dehydrogenase. $^{*}P < 0.05$, $^{**}P < 0.01$, $^{***}P < 0.001$

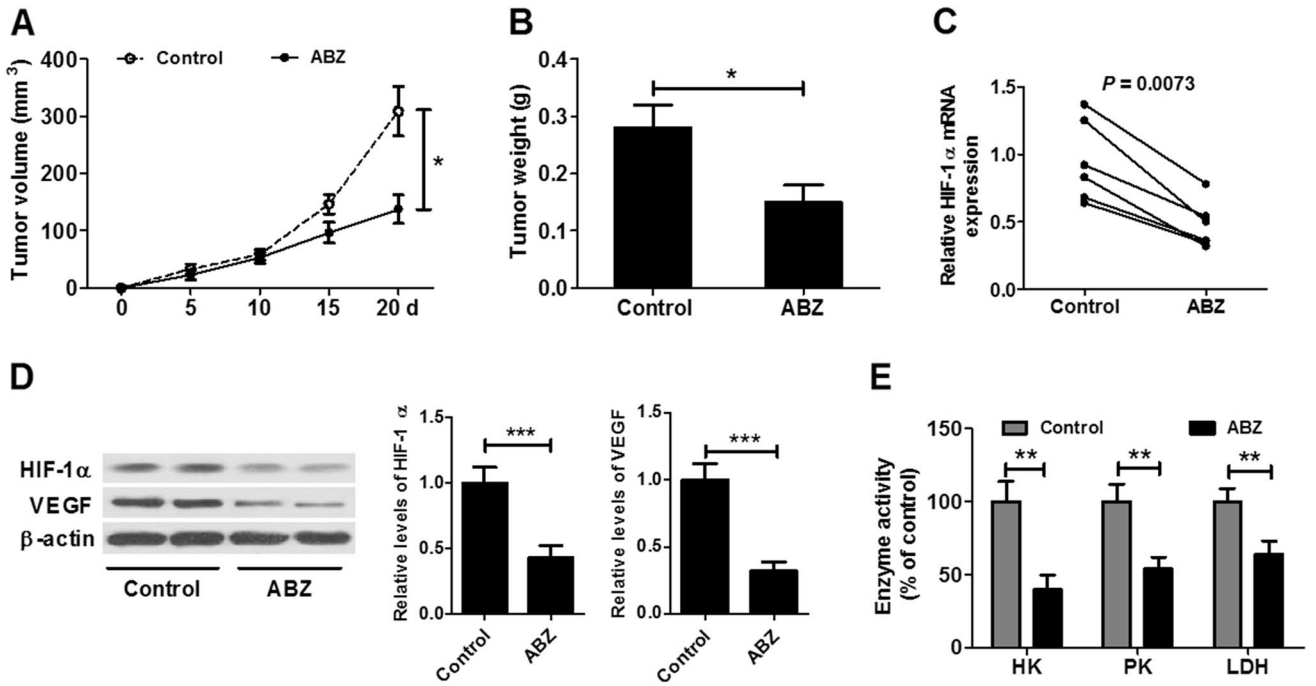

Fig. 4 ABZ inhibited A549 xenograft growth in mouse models. **a, b** ABZ inhibited the tumor volume and weight of A549 xenograft growth in mouse models. A549 were subcutaneously injected into the flank of nude mice. The control group received vehicle and the ABZ group was administered 50 mg/kg of ABZ. Both the groups received the treatment intraperitoneally every 3 days, and tumor volume was measured and calculated every 5 days. After 20 days, the animals were sacrificed and the tumors were harvested and weighted. **c, d** ABZ inhibited HIF-1α mRNA and protein and VEGF expression in A549 xenografts in mouse models. HIF-1α mRNA was detected using qRT-PCR and protein expression levels of HIF-1α and VEGF were detected using western blot. **e** ABZ decreased the activities of HK, PK, and LDH in A549 xenografts. The activities of HK, PK, and LDH were detected by colorimetric assay using specific test kit. Data are shown as mean ± SD ($n = 6$). *HK* hexokinase, *PK* pyruvate kinase, *LDH* lactate dehydrogenase. $^{*}P < 0.05$, $^{**}P < 0.01$, $^{***}P < 0.001$

HIF-1α expression in a dose-dependent manner [32], which is consistent with our study. PX-478 suppresses the levels of hypoxia-induced HIF-1α in cancer cells [33, 34]. Our result showed that PX-478 inhibited HIF-1α and resulted in reduction of VEGF expression in NSCLC A549 cells, which demonstrated that VEGF expression is HIF-1α-dependent in NSCLC A549 cells. Targeting HIF-1α may be a potential treatment for NSCLC.

Anaerobic glycolysis is important for the energy production and low-pH environment maintenance in tumor. Luo et al. [35] found that HIF-1α acts as a switch for oxygen regulation in glucose metabolism by regulating the expression and activity of pyruvate kinase muscle isozyme 2 (PKM2) in cancer cells. There are some critical enzymes in glycolysis, such as HK, LDH, and PK. HK catalyzes six-carbon sugars into hexose phosphate and is a rate-limiting enzyme in glycolysis. LDH converts pyruvate to lactate and acidizes the tumor microenvironment, which would benefit the tumor. PK catalyzes the transfer of phosphoenolpyruvate into pyruvate, which is upstream of the decisive point for glycolytic or oxidative metabolism [36]. Inhibition of glycolysis can block the energy source of tumor cells thus suppressing the tumor development. Sanchez et al. [37] found that dichloroacetate induced growth reduction in multiple myeloma cells by inhibiting aerobic glycolysis. In lung cancer cells, p53 suppressed hypoxia-stimulated glycolysis through Ras-related associated with diabetes (RRAD), which inhibits GLUT1 translocation to the plasma membrane and represses glycolysis [38]. Knockdown glycometabolic proteins using siRNA could also downregulate glycolysis and inhibit proliferation of tumor cells [39]. It is reported that ABZ not only blocks the ATP formation by inhibiting the fumaric reductase system, but also depletes glycogen storage and inhibits glucose absorption in parasite [40, 41]. The exactly mechanism of ABZ inhibits glycolysis in tumor cells remains unknown. In our study, we found that ABZ suppressed HK, PK, LDH activities and lactate production in A549 cells, indicating glycolysis pathway in A549 cells was inhibited by ABZ. Furthermore, our results showed that inhibition of HIF-1α by PX-478 resulted in reduction of glycolysis. It demonstrated that HIF-1α could influence the activities of HK, PK, LDH, and the lactate production and glycolysis is HIF-1α-dependent in NSCLC A549 cells. We speculate that ABZ suppresses glycolysis by inhibiting HIF-1α expression.

In conclusion, our results suggested that ABZ inhibited HIF-1α-dependent glycolysis and VEGF expression in NSCLC cells. Our *in vivo* experiments supported that ABZ may be an important candidate for anti-cancer therapy of NSCLC. Researching on the inhibitory mechanism of ABZ on NSCLC lays a theoretical foundation for combination drug therapy.

Acknowledgements We thank all the members in our department for their help in experiment methods suggestion and data collection.

Compliance with ethical standards

Conflict of interest All authors declared that no competing interests existed.

References

1. Chen W, Zheng R, Baade PD, Zhang S, Zeng H, Bray F, Jemal A, Yu XQ, He J (2016) Cancer statistics in China, 2015. CA Cancer J Clin 66(2):115–132
2. Siegel R, Miller K, Jemal A (2015) Cancer statistics, 2015. CA Cancer J Clin 65(1):5–29
3. Horton J (2002) Albendazole: a broad spectrum anthelminthic for treatment of individuals and populations. Curr Opin Infect Dis 15(6):599–608
4. Lacey E (1990) Mode of action of benzimidazoles. Parasitol Today 6(4):112–115
5. Lacey E, Watson TR (1985) Activity of benzimidazole carbamates against L1210 mouse leukaemia cells: correlation with in vitro tubulin polymerization assay. Biochem Pharmacol 34(19):3603–3605
6. Pourgholami M, Woon L, Almajd R, Akhter J, Bowery P, Morris D (2001) In vitro and in vivo suppression of growth of hepatocellular carcinoma cells by albendazole. Cancer Lett 165(1):43–49
7. Pourgholami MH, Akhter J, Wang L, Lu Y, Morris DL (2005) Antitumor activity of albendazole against the human colorectal cancer cell line HT-29: in vitro and in a xenograft model of peritoneal carcinomatosis. Cancer Chemother Pharmacol 55(5):425–432
8. Pourgholami MH, Szwajcer M, Chin M, Liauw W, Seef J, Galettis P, Morris DL, Links M (2010) Phase I clinical trial to determine maximum tolerated dose of oral albendazole in patients with advanced cancer. Cancer Chemother Pharmacol 65(3):597–605
9. Kim JW, Dang CV (2006) Cancer's molecular sweet tooth and the Warburg effect. Cancer Res 66(18):8927–8930
10. Alfarouk KO, Muddathir AK, Shayoub ME (2011) Tumor acidity as evolutionary spite. Cancers 3(1):408–414
11. Cairns RA, Harris IS, Mak TW (2011) Regulation of cancer cell metabolism. Nat Rev Cancer 11(2):85–95
12. Semenza GL (2010) HIF-1: upstream and downstream of cancer metabolism. Curr Opin Genet Dev 20(1):51–56
13. Denko NC (2008) Hypoxia, HIF1 and glucose metabolism in the solid tumour. Nat Rev Cancer 8(9):705–713
14. Jaakkola P, Mole DR, Tian YM, Wilson MI, Gielbert J, Gaskell SJ, von Kriegsheim A, Hebestreit HF, Mukherji M, Schofield CJ (2001) Targeting of HIF-α to the von Hippel-Lindau ubiquitylation complex by O2-regulated prolyl hydroxylation. Science 292(5516):468–472
15. Ahluwalia A, S Tarnawski A (2012) Critical role of hypoxia sensor-HIF-1α in VEGF gene activation. Implications for angiogenesis and tissue injury healing. Curr Med Chem 19(1):90–97
16. Cathcart MC, Gately K, Cummins R, Drakeford C, Kay EW, O'Byrne KJ, Pidgeon GP (2014) Thromboxane synthase expression and correlation with VEGF and angiogenesis in non-small cell lung cancer. Biochim Biophys Acta 1842(5):747–755
17. Alevizakos M, Kaltsas S, Syrigos KN (2013) The VEGF pathway in lung cancer. Cancer Chemother Pharmacol 72(6):1169–1181
18. Okumura H, Uchikado Y, Setoyama T, Matsumoto M, Owaki T, Ishigami S, Natsugoe S (2014) Biomarkers for predicting the response of esophageal squamous cell carcinoma to neoadjuvant chemoradiation therapy. Surg Today 44(3):421–428
19. Shiau AL, Shen YT, Hsieh JL, Wu CL, Lee CH (2014) Scutellaria barbata inhibits angiogenesis through downregulation of HIF-1 α in lung tumor. Environ Toxicol 29(4):363–370
20. Ahn GO, Seita J, Hong BJ, Kim YE, Bok S, Lee CJ, Kim KS, Lee JC, Leeper NJ, Cooke JP, Kim HJ, Kim IH, Weissman IL, Brown JM (2014) Transcriptional activation of hypoxia-inducible factor-1 (HIF-1) in myeloid cells promotes angiogenesis through VEGF and S100A8. Proc Natl Acad Sci USA 111(7):2698–2703
21. Noorani L, Stenzel M, Liang R, Pourgholami MH, Morris DL (2015) Albumin nanoparticles increase the anticancer efficacy of albendazole in ovarian cancer xenograft model. J Nanobiotechnol 13(1):25
22. Patel K, Doudican NA, Schiff PB, Orlow SJ (2011) Albendazole sensitizes cancer cells to ionizing radiation. Radiat Oncol 6:160
23. Liu JS, Liu J (2013) Effect of Albendazole on proliferation and apoptosis of human colon carcinoma SW480 cells and Bcl-2 expression. Chin J Biol 26(5):685–689
24. Clara CA, Marie SK, Almeida JRW, Wakamatsu A, Oba-Shinjo SM, Uno M, Neville M, Rosemberg S (2014) Angiogenesis and expression of PDGF-C, VEGF, CD105 and HIF-1α in human glioblastoma. Neuropathology 34(4):343–352
25. Saharinen P, Eklund L, Pulkki K, Bono P, Alitalo K (2011) VEGF and angiopoietin signaling in tumor angiogenesis and metastasis. Trends Mol Med 17(7):347–362
26. Lee JK, Park SR, Jung BK, Jeon YK, Lee YS, Kim MK, Kim YG, Jang JY, Kim CW (2013) Exosomes derived from mesenchymal stem cells suppress angiogenesis by down-regulating VEGF expression in breast cancer cells. PLoS ONE 8(12):e84256
27. Noorani L, Stenzel M, Liang R, Pourgholami MH, Morris DL (2015) Albumin nanoparticles increase the anticancer efficacy of albendazole in ovarian cancer xenograft model. J Nanobiotechnology 13:25
28. Pourgholami MH, Cai ZY, Badar S, Wangoo K, Poruchynsky MS, Morris DL (2010) Potent inhibition of tumoral hypoxia-inducible factor 1α by albendazole. BMC Cancer 10(1):143
29. Pourgholami MH, Cai ZY, Lu Y, Wang L, Morris DL (2006) Albendazole: a potent inhibitor of vascular endothelial growth factor and malignant ascites formation in OVCAR-3 tumor-bearing nude mice. Clin Cancer Res 12(6):1928–1935
30. Giatromanolaki A, Koukourakis MI, Sivridis E, Turley H, Talks K, Pezzella F, Gatter KC, Harris AL (2001) Relation of hypoxia inducible factor 1α and 2α in operable non-small cell lung cancer to angiogenic/molecular profile of tumours and survival[J]. Br J Cancer 85(6):881–890
31. Guo M, Song L-P, Jiang Y, Liu W, Yu Y, Chen G-Q (2006) Hypoxia-mimetic agents desferrioxamine and cobalt chloride induce leukemic cell apoptosis through different hypoxia-inducible factor-1α independent mechanisms. Apoptosis 11(1):67–77
32. Borcar A, Menze MA, Toner M, Hand SC (2013) Metabolic preconditioning of mammalian cells: mimetic agents for hypoxia

lack fidelity in promoting phosphorylation of pyruvate dehydrogenase. Cell Tissue Res 351(1):99–106
33. Koh MY, Spivak-Kroizman T, Venturini S, Welsh S, Williams RR, Kirkpatrick DL, Powis G (2008) Molecular mechanisms for the activity of PX-478, an antitumor inhibitor of the hypoxia-inducible factor-1α. Mol Cancer Ther 7(1):90–100
34. Welsh S, Williams R, Kirkpatrick L, Paine-Murrieta G, Powis G (2004) Antitumor activity and pharmacodynamic properties of PX-478, an inhibitor of hypoxia-inducible factor-1α. Mol Cancer Ther 3(3):233–244
35. Luo W, Hu H, Chang R, Zhong J, Knabel M, O'Meally R, Cole RN, Pandey A, Semenza GL (2011) Pyruvate kinase M2 is a PHD3-stimulated coactivator for hypoxia-inducible factor 1. Cell 145(5):732–744
36. Luo W, Semenza GL (2011) Pyruvate kinase M2 regulates glucose metabolism by functioning as a coactivator for hypoxia-inducible factor 1 in cancer cells. Oncotarget 2(7):551–556
37. Sanchez W, McGee S, Connor T, Mottram B, Wilkinson A, Whitehead J, Vuckovic S, Catley L (2013) Dichloroacetate inhibits aerobic glycolysis in multiple myeloma cells and increases sensitivity to bortezomib. Brit. J Cancer 108(8):1624–1633
38. Zhang C, Liu J, Wu R, Liang Y, Lin M, Liu J, Chan CS, Hu W, Feng Z (2014) Tumor suppressor p53 negatively regulates glycolysis stimulated by hypoxia through its target RRAD. Oncotarget 5(14):5535–5546
39. Su J, Chen X, Kanekura T (2009) A CD147-targeting siRNA inhibits the proliferation, invasiveness, and VEGF production of human malignant melanoma cells by down-regulating glycolysis. Cancer Lett 273(1):140–147
40. Wang J, Qi H, Diao Z, Zheng X, Li X, Ma S, Ji A, Yin C (2010) An outbreak of angiostrongyliasis cantonensis in Beijing. J Parasitol 96(2):377–381
41. Vinaud MC, Ferreira CS, Junior RdSL, Bezerra JCB (2008) Taenia crassiceps: energetic and respiratory metabolism from cysticerci exposed to praziquantel and albendazole in vitro. Exp Parasitol 120(3):221–226